Nonmonotonic residual entropy in diluted spin ice: A comparison between Monte Carlo simulations of diluted dipolar spin ice models and experimental results

T. Lin,[1] X. Ke,[2,3,4] M. Thesberg,[1,5] P. Schiffer,[2,6] R. G. Melko,[1,7] and M. J. P. Gingras[1,7,8]

[1]*Department of Physics and Astronomy, University of Waterloo, Waterloo, Ontario, Canada N2L 3G1*

[2]*Department of Physics and Materials Research Institute, Pennsylvania State University, University Park, Pennsylvania 16802, USA*

[3]*Quantum Condensed Matter Division, Oak Ridge National Laboratory, Oak Ridge, Tennessee 37831, USA*

[4]*Department of Physics and Astronomy, Michigan State University, East Lansing, Michigan 48824, USA*

[5]*Department of Physics and Astronomy, McMaster University, Hamilton, Ontario, Canada L8S 4M1*

[6]*Department of Physics and Frederick Seitz Materials Research Laboratory, The University of Illinois at Urbana-Champaign, 1110 West Green Street, Urbana, Illinois 61801-3080, USA*

[7]*Perimeter Institute for Theoretical Physics, 31 Caroline North, Waterloo, Ontario, Canada N2L-2Y5*

[8]*Canadian Institute for Advanced Research, 180 Dundas Street West, Suite 1400, Toronto, Ontario, Canada M5G 1Z8*

(Received 25 March 2013; revised manuscript received 15 November 2014; published 19 December 2014)

Spin ice materials, such as $Dy_2Ti_2O_7$ and $Ho_2Ti_2O_7$, are highly frustrated magnetic systems. Their low-temperature strongly correlated state can be mapped onto the proton disordered state of common water ice. As a result, spin ices display the same low-temperature residual Pauling entropy as water ice, at least in calorimetric experiments that are equilibrated over moderately long-time scales. It was found in a previous study [X. Ke *et al.*, Phys. Rev. Lett. **99**, 137203 (2007)] that, upon dilution of the magnetic rare-earth ions (Dy^{3+} and Ho^{3+}) by nonmagnetic yttrium (Y^{3+}) ions, the residual entropy depends *nonmonotonically* on the concentration of Y^{3+} ions. A quantitative description of the magnetic specific heat of site-diluted spin ice materials can be viewed as a further test aimed at validating the microscopic Hamiltonian description of these systems. In this work, we report results from Monte Carlo simulations of site-diluted microscopic dipolar spin ice models (DSIM) that account quantitatively for the experimental specific-heat measurements, and thus also for the residual entropy, as a function of dilution, for both $Dy_{2-x}Y_xTi_2O_7$ and $Ho_{2-x}Y_xTi_2O_7$. The main features of the dilution physics displayed by the magnetic specific-heat data are quantitatively captured by the diluted DSIM up to 85% of the magnetic ions diluted ($x = 1.7$). The previously reported departures in the residual entropy between $Dy_{2-x}Y_xTi_2O_7$ versus $Ho_{2-x}Y_xTi_2O_7$, as well as with a site-dilution variant of Pauling's approximation, are thus rationalized through the site-diluted DSIM. We find for 90% ($x = 1.8$) and 95% ($x = 1.9$) of the magnetic ions diluted in $Dy_{2-x}Y_xTi_2O_7$ a significant discrepancy between the experimental and Monte Carlo specific-heat results. We discuss possible reasons for this disagreement.

DOI: 10.1103/PhysRevB.90.214433 PACS number(s): 75.10.Hk, 05.50.+q, 75.40.Mg, 75.50.Lk

I. INTRODUCTION

One of the most interactive collaborations in contemporary condensed matter physics occurs in the theoretical and experimental study of geometrically frustrated magnets [1–6]. In these systems, the predominant microscopic interactions compete with each other, inhibiting the development of long-range magnetic order down to very low, if not zero, temperature [5]. The temperature regime where strong magnetic correlations exist, but long-range order is absent, is commonly referred to as spin liquid or cooperative paramagnetic state [7], where collective excitations can give rise to exotic behavior unique to such frustrated systems [5]. Since the connection between theoretical predictions and experimental signatures of such novel phenomena is still under exploration, the continuing dialog between theory and experiment is crucial in order to maintain the rapid pace of development in the field.

Particularly successful exchanges between theory and experiment in geometrically frustrated magnetism are found in the study of spin ice materials [3,4,6,8,9]. These are realized by the canonical compounds $Dy_2Ti_2O_7$ [9], $Ho_2Ti_2O_7$ [8], and the less extensively studied $Dy_2Sn_2O_7$ [10] and $Ho_2Sn_2O_7$ [11]. More recently, $Dy_2Ge_2O_7$ and $Ho_2Ge_2O_7$ have been made through high-pressure chemical synthesis, and shown to be spin ice systems through thermodynamic measurements [12,13], as has $CdEr_2Se_4$, in which, unusually, Er^{3+} is described by an Ising spin [14]. In all of these materials, the magnetic rare-earth Dy^{3+}, Ho^{3+}, and Er^{3+} ions sit on the vertices of a pyrochlore lattice of corner-sharing tetrahedra; the Ti^{4+}, Sn^{4+}, and Ge^{4+} ions are nonmagnetic. Because of the very large single-ion anisotropy in these systems, the moments can be described below a temperature $T \sim 50$ K as classical Ising spins pointing along their local [111] direction at their respective pyrochlore lattice sites [8,15,16]. Below a typical temperature of order 1 K, the magnetic state of $(Dy,Ho)_2(Ti,Sn,Ge)_2O_7$ can be mapped onto the proton disordered state of common water ice [17], hence, the name spin ice [8]. In this low-temperature spin ice state, the magnetic moments are highly constrained locally and obey the so-called "ice rules": two spins point in and two spins point out of each tetrahedron of the pyrochlore lattice, but without displaying long-range order [3]. This constraint leads the spin ice state to be viewed as a cooperative paramagnet [7] or a *classical spin liquid* [5], a label that stems from the very strong Ising nature of the lowest-energy crystal-field doublet for both Dy^{3+} and Ho^{3+} and results in a dramatically reduced level of quantum spin dynamics [16]. At the same time, the high-energy barrier to single spin flips causes the relaxation dynamics to become very slow in these materials below $T \sim 1$ K. Consequently, spin ices should be viewed as extremely sluggish classical spin liquids [18].

Remarkably, the question of slow dynamics in frustrated icelike systems has been previously considered in the original context of water ice, where extensive calorimetric studies were carried out long before [19,20] its magnetic counterparts were discovered [8]. The nature of the proton disorder in ice was described by Pauling who estimated the residual entropy to be $S_P = R/2 \ln(3/2)$ per mole of protons (R is the molar gas constant) [17], matching closely with experiments [19,20]. However, as water ice is doped with alkali hydroxides, such as KOH or RbOH, a sharp first-order transition to long-range order occurs at a temperature near 72 K. At that transition, a large portion of the residual Pauling entropy is released through the latent heat [21,22]. These experiments suggest that the proton disordered ice state is somewhat fragile against impurities and that the frustrated disordered ice state with residual entropy can be eliminated through the influence of impurities and/or random disorder. Yet, despite much theoretical work, it remains unclear as to what is the exact mechanism via which alkali hydroxides in the water ice system promotes the development of long-range order [23] and what role the impurities play on slow dynamical processes.

Inspired by the impurity-driven long-range order observed in water ice [21,22], one may ask whether the magnetic spin ice analog could also display interesting behavior when subject to the addition of random impurities. As discussed above, a Pauling residual entropy is generically found in undiluted spin ice materials [9,10,13,14,24,25]. See, however, Ref. [26] where no residual Pauling entropy plateau is found in $Dy_2Ti_2O_7$ if extraordinary long relaxation time scales of several days is afforded below a temperature of order of 0.4 K. We return to this issue later in this Introduction. The most prominent thermodynamic indicator that the above materials enter a correlated spin ice state is the broad specific-heat peak at the "peak temperature" T^{peak}, with $T^{\text{peak}} \sim 1.1$ K for $Dy_2Ti_2O_7$ [9,26,27] and $T^{\text{peak}} \sim 1.9$ K for $Ho_2Ti_2O_7$ [27,28]. There is no thermodynamic phase transition between the high-temperature paramagnetic state and the low-temperature spin ice state as evidenced by the absence of sharp thermodynamic features at T^{peak}. Theoretical studies have shown that long-range magnetostatic dipole-dipole interactions are responsible for the ice rule obeying spin ice state in $(Ho,Dy)_2(Ti,Sn,Ge)_2O_7$ compounds [28–32]. Yet, the same dipolar interactions should give rise to long-range order [30,31] at a critical temperature $T_c \ll T^{\text{peak}}$ if true thermal equilibrium can be maintained, as observed in Monte Carlo simulations of a simple dipolar spin ice model (DSIM) [29] that employ nonlocal loop moves [33,34]. To date, however, no experiment has found a transition to long-range order in spin ice materials [26,35], presumably because of a dynamical arrest in spin flips [36] and the associated relaxation times growing exponentially fast below a temperature of about 1 K [26,37].

Hence, it is perhaps reasonable to imagine that a slight dilution of the magnetic Dy^{3+} and Ho^{3+} ions could lower the kinematic barriers for spin flips, thus accelerating the spin dynamics, and help promote a transition to long-range order without significantly affecting the broken discrete symmetry long-range ordered ground state of dipolar spin ice [33,34]. Luckily, magnetic site dilution in spin ices can be realized rather straightforwardly in the $Dy_{2-x}Y_xTi_2O_7$ and $Ho_{2-x}Y_xTi_2O_7$ compounds. These form a solid solution over the whole $x \in [0,2]$ range where the magnetic Dy^{3+} and Ho^{3+} ions are replaced by nonmagnetic Y^{3+} ions [27]. The close ionic radius of Y^{3+} with that of Dy^{3+} and Ho^{3+} allow for a substitution causing negligible local lattice deformation and strain [6], similarly to the situation in the $LiHo_{1-x}Y_xF_4$ dipolar Ising ferromagnet [38–43]. In such a situation, the substitution of Dy^{3+}/Ho^{3+} by Y^{3+} in $Dy_{2-x}Y_xTi_2O_7$ and $Ho_{2-x}Y_xTi_2O_7$ can thus be viewed as the mere removal of the Dy^{3+}/Ho^{3+} magnetic species. The study of site-diluted spin ices may thus offer a unique opportunity to investigate quantitatively the effect of random disorder in a strongly correlated (classical) spin-liquid state. Such an endeavor should be achievable by noting, for example, the quantitative progress made in describing the thermodynamic properties of the $LiHo_{1-x}Y_xF_4$ dipolar Ising system, both in the diluted-ferromagnetic regime [39,40] as well as in the dipolar spin-glass regime [38–43].

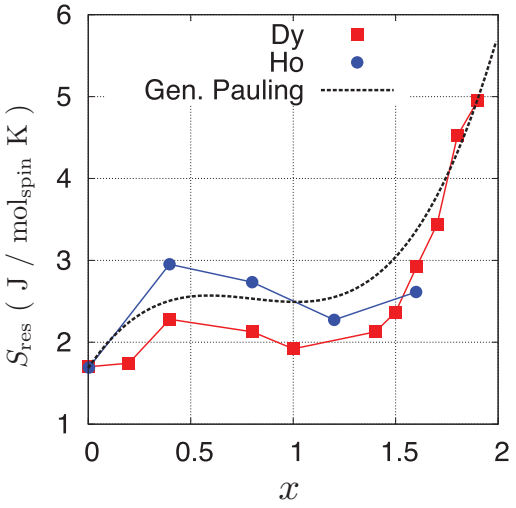

FIG. 1. (Color online) Experimental residual entropy as a function of dilution level x for the $Dy_{2-x}Y_xTi_2O_7$ and $Ho_{2-x}Y_xTi_2O_7$ compounds (adapted from Ke *et al.* [27]) . Dy denotes $Dy_{2-x}Y_xTi_2O_7$, Ho denotes $Ho_{2-x}Y_xTi_2O_7$, and Gen. Pauling denotes the generalized Pauling approximation (gPa) presented in Ref. [27]. As noted by Ke *et al.*, there is an obvious departure between the three curves, except for the undiluted compounds ($x = 0$).

A neutron scattering study shows no sign of long-range ordering in $Ho_{2-x}Y_xTi_2O_7$ down to 30 mK for $x = 0.3$ and 1.0 [44]. On the other hand, specific-heat measurements have found that the low-temperature residual entropy $S_{\text{res}}(x)$ of diluted $Dy_{2-x}Y_xTi_2O_7$ and $Ho_{2-x}Y_xTi_2O_7$ spin ices display a nonmonotonic dependence on the level of dilution x [27]. This dependence of $S_{\text{res}}(x)$ on x is actually accompanied by a nonmonotonous x dependence of the temperature $T^{\text{peak}}(x)$ at which the magnetic specific heat $C_m(T)$ peaks and reaches the peak value $C_m^{\text{peak}}(x)$ (see Fig. 2). We return to this point in the next paragraph. A calculation generalizing Pauling's argument [17] (gPa) to the case of site dilution of a nearest-neighbor spin ice model [8] also finds a nonmonotonic behavior of $S_{\text{res}}(x)$ (see dashed curve in Fig. 1) [27]. However, the apparent systematic departures between the gPa and the experiment results as well as the differences between Dy- and Ho-based materials (see Fig. 1) have so far remained unaddressed. It was suggested in the original work [27] that the residual

entropy may be material dependent and have a more drastic nonmonotonic dependence on levels of dilution than the gPa does. The reason for such differences being caused, for example, by the extra complexities (e.g., long-range nature) of the dipolar interactions compared with the nearest-neighbor spin ice model. One of the main goals of this work is to identify precisely how this difference between the gPa and the experimental results arise.

There is, apart from wanting to rationalize the difference in $S_{\rm res}(x)$ between $Dy_{2-x}Y_xTi_2O_7$ and $Ho_{2-x}Y_xTi_2O_7$ as well as with the gPa, another important motivation for investigating the dilution dependence of the currently available dipolar spin ice models for $Dy_2Ti_2O_7$ [45] and $Ho_2Ti_2O_7$ [28]. As mentioned above, Ref. [26] finds below $T \sim 0.45$ K a dramatically different behavior compared to that found in all prior $C_{\rm m}(T)$ measurements on $Dy_2Ti_2O_7$. These new results may possibly be viewed as a challenge to the dipolar spin ice model (DSIM) description of this material [29,45]. To address this question, one may ask whether the low-energy scale responsible for this recently reported low-temperature behavior could be exposed in experiments where the currently available DSIM Hamiltonian is being tested in a regime of parameters (e.g., magnetic field, dilution, etc.) far from the one for which it was originally designed [28,29,45]. As the specific-heat peak features $T^{\rm peak}(x)$ and $C_{\rm m}^{\rm peak}(x)$ signal the underlying condensation of the two-in/two-out ice rule defects (i.e., "monopoles" [32]) upon cooling, the x dependence of $T^{\rm peak}(x)$ and $C_{\rm m}^{\rm peak}(x)$ informs us on the evolution of the ice-rule correlations as a function of x. Hence, an ultimately successful quantitative description of $T^{\rm peak}(x)$ and $C_{\rm m}^{\rm peak}(x)$ would provide a further and seemingly compelling demonstration that the microscopic spin Hamiltonian at hand [45], including its Ising nature, is robust against a large departure from its original design setting.

In order to investigate the microscopic origin of the relative departure of the three curves in Fig. 1 as well as the x dependence of $T^{\rm peak}(x)$ and $C_{\rm m}^{\rm peak}(x)$ in Fig. 2, we have performed Monte Carlo simulations of a diluted variant of the pertinent microscopic dipolar spin ice model of $Ho_2Ti_2O_7$ [28] and $Dy_2Ti_2O_7$ [45]. A direct comparison of the temperature-dependent magnetic specific heat $C_{\rm m}(T)$ for various dilution levels x between simulations and experiments is made in order to validate a simple site-diluted version of the otherwise pure (dilution-free) microscopic models. Through the simulation data, we obtain an accurate $C_{\rm m}(T)$ which provides for a precise determination of the residual entropy, down to the lowest temperature $T_0 \sim 0.4$ K considered in the experiments of Ke *et al.* in Ref. [27] on diluted $Dy_{2-x}Y_xTi_2O_7$ and $Ho_{2-x}Y_xTi_2O_7$.

The three main conclusions of our work are as follows. First, we find that a DISM with simple site dilution is able to describe quantitatively well $C_{\rm m}(T)$ for $Dy_{2-x}Y_xTi_2O_7$ and $Ho_{2-x}Y_xTi_2O_7$ in the temperature range $T \in [0.5,5.0]$ K *without any adjustment* of the Hamiltonian available for the dilution-free variants of these two materials [28,45]. For example, Fig. 2 illustrates this for the case of $Dy_{2-x}Y_xTi_2O_7$. Second, our simulation results confirm the previous speculation [27] that the material-dependent residual entropy originates from the material-specific details of the interactions. Specifically, it is due to the fact that $Dy_{2-x}Y_xTi_2O_7$ and $Ho_{2-x}Y_xTi_2O_7$ have a ratio of their dipolar interaction energy scale to the nearest-neighbor antiferromagnetic exchange coupling that differs by a factor of about 2. Furthermore, the failure of the gPa to describe quantitatively the residual entropy of diluted dipolar spin ice materials and models is inconsistent with the notion of projective equivalence [31,32] which associates the low-temperature regime of the DISM to an effective nearest-neighbor spin ice model. Finally, our conclusion regarding the different residual entropy $S_{\rm res}$ of $Ho_2Ti_2O_7$ and $Dy_2Ti_2O_7$ differs from the one reached in Ref. [27] and illustrated in Fig. 1. Namely, we find that $Ho_{2-x}Y_xTi_2O_7$ has a smaller $S_{\rm res}(x)$ than $Dy_{2-x}Y_xTi_2O_7$ does for any experimental baseline temperature value T_0 chosen identical for the two sets of compounds.

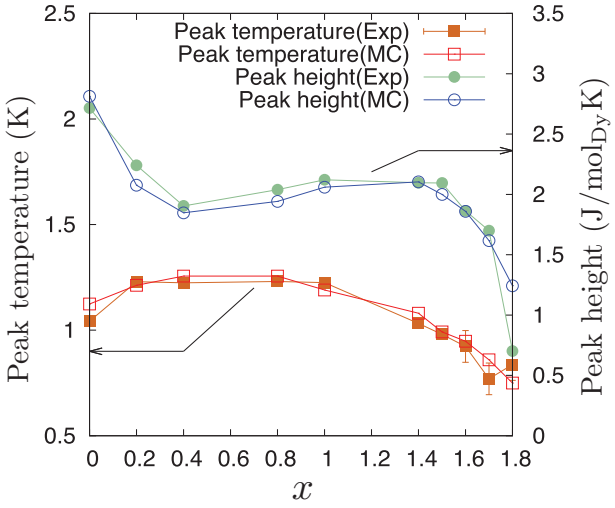

FIG. 2. (Color online) Dilution x, dependence of the peak height $C_{\rm m}^{\rm peak}(x)$, and peak temperature $T^{\rm peak}(x)$ of the magnetic specific heat $C_{\rm m}(T)$ of $Dy_{2-x}Y_xTi_2O_7$. The closed symbols show experimental data while the open symbols are from Monte Carlo simulations of a site-diluted dipolar spin ice model (see text). The circles show the x dependence of $C_{\rm m}^{\rm peak}(x)$ (right axis) while the squares show x dependence of $T^{\rm peak}(x)$ on the left axis. A nonmonotonic dependence of $C_{\rm m}^{\rm peak}(x)$ and $T^{\rm peak}(x)$ as a function of x is clearly seen in both the experimental and Monte Carlo data. The good agreement between experimental and Monte Carlo data for *both* quantities that we establish in this work shows that the hypothesis of a simple site-diluted dipolar spin ice model (DSIM) describing $Dy_{2-x}Y_xTi_2O_7$ is reasonably well confirmed up to $x = 1.8$. This is one of the main conclusions of our work.

The rest of the paper is organized as follows: In Sec. II, we discuss the details of the experimental methods. In Sec. III, we present our microscopic models and the Monte Carlo simulation methods. In Sec. IV, we present and discuss the results of the Monte Carlo simulations and address the previously reported [27] material-dependent residual entropies along with their departure from the gPa predictions. Finally, Sec. V concludes the paper.

II. EXPERIMENTAL METHODS AND RESULTS

Specific-heat $C(T)$ measurements were performed on Y-diluted spin ice materials $Dy_{2-x}Y_xTi_2O_7$ and $Ho_{2-x}Y_xTi_2O_7$ using a Quantum Design Physical Property Measurement

System (PPMS) cryostat with the He3 option via a standard semiadiabatic heat pulse technique. The Dy-based samples were thoroughly mixed with silver (Ag) and pressed into pellets to facilitate thermal equilibration. The scaled Ag specific heat, measured separately, was subtracted from the total specific heat. Generally, a few tens mg of Ag were mixed with roughly similar amount of Dy-based powders (both were measured with 0.1 mg error) and ground together. At the end, pellets with a mass of $10 \sim 20$ mg were measured. The phonon contribution was extracted by fitting the data with the Debye formula in the temperature range $T \in [10,20]$ K, and subtracted from the total specific heat to obtain the magnetic specific-heat contribution $C_{\rm m}(T)$. Ho-based samples were pressed directly into pellets and the magnetic specific heat was obtained after subtracting both the phonon and the large Ho nuclear Schottky anomaly contribution [24,28]. The data $C_{\rm m}(T)/T$ integrated from $\tilde{T}_0(x) = 0.4 \pm 0.1$ K, depending on the lowest temperature $\tilde{T}_0(x)$ experimentally accessed for a given concentration x, up to a ("high") temperature $T \gg T^{\rm peak}(x)$, was used to determine the residual low-temperature entropy $S_{\rm res}(\tilde{T}_0)$, reported. As discussed in the Introduction, this experimentally determined residual entropy $S_{\rm res}(\tilde{T}_0)$, reported in Ref. [27] and plotted in Fig. 1, varies nonmonotonically as a function of the Y concentration for both the $Dy_{2-x}Y_xTi_2O_7$ and the $Ho_{2-x}Y_xTi_2O_7$ series, being very roughly qualitatively captured by a generalization of Pauling approximation's (gPa) that is represented by the dashed curve in Fig. 1 above [27].

III. MICROSCOPIC MODELS AND MONTE CARLO SIMULATIONS

A. Microscopic models of spin ices

In spin ices, the magnetic moments reside on a pyrochlore lattice, which consists of a face-centered-cubic lattice of corner-sharing tetrahedra primitive units [3,6]. Due to the large energy scale ($\sim$300 K) of the crystal field splitting between the ground-state doublet and the lowest-energy excited doublet that exist in $Dy_2Ti_2O_7$ and $Ho_2Ti_2O_7$ [6,15,16], the states that form the ground doublet of the Dy^{3+} and Ho^{3+} ions can safely be assumed to be the only thermodynamically relevant states below a temperature $T \lesssim 50$ K.

As suggested originally [8], the minimal model that describes the geometrical frustration in spin ices is

$$\mathcal{H}_{\rm NNSIM} = J_{\rm eff} \sum_{\langle i,j \rangle} \sigma_i \sigma_j, \tag{1}$$

where $J_{\rm eff} > 0$ is the effective antiferromagnetic interaction between the σ's Ising variables. This model possesses a Pauling residual entropy $S_{\rm P}$ [46] and displays at zero temperature an ice-rule-obeying ground state characterized by dipolarlike spin-spin correlations that emerge from the "two-in/two-out" ice-rule constraint [47–49].

On the other hand, in real spin ice materials, the Dy^{3+} and Ho^{3+} ions carry a large magnetic moment ($\sim 10\mu_{\rm B}$) and the long-range dipolar interactions cannot be ignored [29–31,50]. Given the symmetry of the crystal field ground state [8,15,16], the magnetic moments can be well described by vector spins constrained by the single-ion anisotropy to point strictly parallel or antiparallel to their respective local [111] direction (i.e., along the line from the corners to the center of each tetrahedron) [3,8,15,16]. Taking the dipolar interaction and the essentially infinite local Ising anisotropy into consideration, the dipolar spin ice model (DSIM) is defined by the Hamiltonian

$$\mathcal{H}_{\rm DSIM} = \sum_{i>j} \sigma_i \sigma_j \left\{ \sum_{\nu=1}^{3} J_\nu \ \delta_{r_{ij},r_\nu} \ \hat{z}_i \cdot \hat{z}_j + D(r_1/r_{ij})^3 [\hat{z}_i \cdot \hat{z}_j - 3(\hat{z}_i \cdot \hat{r}_{ij})(\hat{z}_j \cdot \hat{r}_{ij})] \right\}. \tag{2}$$

The $\sigma_i = \pm 1$ are the Ising spin variables on the pyrochlore lattice. The $\hat{z}_i$ is the local [111] direction of the Ising axis at site i, which points from the corner of a tetrahedron to its center. The first term describes the Ising exchange interaction and the second term is the long-range magnetic dipole-dipole interaction. Here, $\nu = 1$, 2, or 3 refers to first-, second-, or third-nearest neighbors, respectively, where J_ν is the exchange coupling and r_ν is the distance between them. There are two types of third-nearest-neighbor interactions which we do not differentiate [45]. D is the strength of the dipolar interactions at nearest-neighbor distance.

Using the most up-to-date values for J_ν and D, we have with our sign convention of J_ν ($J_\nu > 0$ is antiferromagnetic; $J_\nu < 0$ is ferromagnetic): $J_1 = 3.41$ K, $J_2 = -0.14$ K, $J_3 = 0.025$ K, and $D = 1.32$ K for $Dy_{2-x}Y_xTi_2O_7$ [45] and $J_1 = 1.56$ K and $D = 1.41$ K for $Ho_{2-x}Y_xTi_2O_7$ [28]. Unfortunately, because of the complexity introduced by the large hyperfine coupling interactions in Ho-based materials [28], much less systematic calorimetric measurements, which provide many of the constraints to determine J_1 and J_2 [45], have not been carried out on $Ho_2Ti_2O_7$ compared to $Dy_2Ti_2O_7$. Consequently, the J_2 and J_3 values for $Ho_2Ti_2O_7$ have not yet been determined [28] and we therefore set $J_2 = J_3 = 0$ for this compound. As we shall see in the following, it turns out that this ($J_2 = J_3 = 0$) model describes well the magnetic specific heat of $Ho_{2-x}Y_xTi_2O_7$ for the $x = 0, 0.4, 0.8,$ and 1.2 values considered in this work. We remind the reader that a rough indicator of the energy scale determining the temperature at which a dipolar spin ice system enters the ice-rule-obeying spin ice regime is set by $J_{\rm eff} \equiv (5D - J_1)/3$ [29]. Here, the factors of 5 and $\frac{1}{3}$ come from the relative orientation of the $\hat{z}_i$ Ising axis ($\hat{z}_i \cdot \hat{z}_j = -\frac{1}{3}$) and the trigonometric factors $(\hat{z}_i \cdot \hat{r}_{ij})(\hat{z}_j \cdot \hat{r}_{ij}) = -\frac{5}{3}$ for nearest neighbors in the second (dipolar) term of Eq. (2). We thus have $J_{\rm eff} = 1.06$ K for $Dy_2Ti_2O_7$ and $J_{\rm eff} = 1.83$ K for $Ho_2Ti_2O_7$.

For the diluted samples, we assume that the nonmagnetic diluting Y^{3+} ions are introduced randomly while *all* other parameters of the material, and therefore those of the model in Eq. (2), are assumed to be unchanged. This means that, until more accurate microscopic or *ab initio* modeling of the effect of diamagnetic site dilution in spin ice compounds becomes available, we ignore local lattice strain effects that may result from the substitution of Dy^{3+} or Ho^{3+} by Y^{3+}. In practice, we thus ignore any changes that may occur in the J_ν exchange couplings, the rare-earth ion magnetic moment μ as well as new quantum transverse spin exchange couplings [51,52] that would all results from a variation of the single-ion crystal field ground-state wave functions. This would seem a reasonable first approximation given the close ionic radius of Y^{3+} with

Dy^{3+} and Ho^{3+}. We note in passing that such an approximation has recently been shown to describe quantitatively quite well the variation of the critical ferromagnetic temperature in Ho^{3+} substituted by Y^{3+} in $LiHo_{1-x}Y_xF_4$ [39–41,43]. In practice, the microscopic J_ν's and D in Eq. (2) are kept to their pure $Dy_2Ti_2O_7$ and $Ho_2Ti_2O_7$ values while the Ising variables are redefined as $\sigma_i \to \epsilon_i\sigma_i$, with $\epsilon_i = 0$ if site i is occupied by nonmagnetic Y^{3+} ion or $\epsilon_i = 1$ if occupied by a magnetic rare-earth ion. Thus, for $(Dy,Ho)_{2-x}Y_xTi_2O_7$, the random site probability distribution of ϵ_i, $P(\epsilon_i)$, is $P(\epsilon_i) = (x/2)\delta(\epsilon_i) + (1 - x/2)\delta(\epsilon_i - 1)$, where $\delta(u)$ is the Dirac delta function.

B. Monte Carlo methods

We carried out Monte Carlo simulations for the above model for $Dy_{2-x}Y_xTi_2O_7$ and $Ho_{2-x}Y_xTi_2O_7$ at various Y^{3+} concentrations x. We used a conventional cubic unit cell containing 16 spins, with the system of linear size L having $16L^3$ spins. Dilution is treated by randomly taking spins out of the system, and a disorder average over 50 different random dilution configurations was performed for each dilution level x. Periodic boundary conditions are used, and we implemented the infinite dipole interactions using the Ewald summation technique [53]. Most of the data production was done with $L = 4$ while, for higher dilutions ($x \geqslant 1.5$), we used $L = 5$ to have a reasonably large number of spins remaining in the system. For most of the results presented in the following, very little system size dependence for the magnetic specific heat $C_m(T)$ was observed.

A conventional single spin-flip Metropolis algorithm was employed for the Monte Carlo simulation. In addition, we used a nonlocal "closed-loop" update [33,34] as well as a new "open-loop" update that we now explain. The open-loop update is a modified version of the closed-loop update with the following amendments. In a diluted system, a fraction of the elementary tetrahedral units will have one or three sites occupied by a spin. Such "± tetrahedra" have the sum of their Ising σ_i variables over the occupied sites equal to ±1 or ±3. At low temperatures, almost all such tetrahedra become constrained to ±1 since these states are energetically lower than the ±3 ones. In terms of the monopole description of the low-temperature spin ice state [36], these ±1 tetrahedra can be viewed as local impurities with fractional ($\pm\frac{1}{2}$) monopole charge.

The open-loop update algorithm searches for an end-to-end chain of spins connecting two of these tetrahedra with opposite sums of the Ising variables. An open-loop update flips all the spins along the chain when accepted. Energetically, the nearest-neighbor part of the $\mathcal{H}_{DSIM}$ is unchanged in such an open-loop Monte Carlo update. We use the term open-loop update to stress the similarity of the algorithm to the original closed-loop update [33,34], but with the chains of the updated spins ending at two "±1 tetrahedra." In order to further facilitate the equilibrium of the system, we found it necessary to also employ the parallel tempering technique which is commonly used in the study of spin-glass models [54]. At least 200 000 Monte Carlo update steps are used with each single-spin-flip update sweep followed by the two types of loop moves update as well as by a parallel tempering replica exchange sweep [54]. Another 200 000 such steps are used for data production. The magnetic specific heat was determined by performing a disorder average of the energy fluctuations:

$$C_m(T) = \frac{[\langle E^2\rangle - \langle E\rangle^2]}{k_B T^2}, \tag{3}$$

where $\langle\ldots\rangle$ and $[\ldots]$ as thermal (Boltzmann) and disorder averages, respectively.

There are two sources of errors in our simulations. One is from the Monte Carlo statistics for each disorder realization. The other is from the sample-to-sample fluctuations for different realizations of sample dilution, which arise in the simulations because we are dealing with a finite-size system. We find the error bars from the Monte Carlo statistics to be typically very small: less than 1% for all cases we checked. This allows us to ignore this type of error and only consider the error from sample-to-sample fluctuations. Therefore, our error bars are given by

$$\sigma = \sqrt{\frac{1}{n-1}([C^2] - [C]^2)}, \tag{4}$$

where $n = 50$ is the number of disorder realizations. For most data points, the error bars are smaller than the width of the solid lines. For the most dilute samples ($x = 1.8$ and 1.9), we have verified, by considering 1000 disorder realizations for $L = 3$, 4, and 5, that the sample-to-sample variation remains well bounded and that there is no Griffiths-type behavior affecting the Monte Carlo specific-heat data, and that $C_m(T)$ is therefore well self-averaged.

IV. RESULTS AND DISCUSSIONS

We plot in Fig. 3 the magnetic specific heat versus temperature $C_m(T)$ obtained from Monte Carlo simulations of Eq. (2) (solid lines) for various levels of dilution in comparison with experimental data (open black circles for $Dy_{2-x}Y_xTi_2O_7$, open red squares for $Ho_{2-x}Y_xTi_2O_7$).

The agreement between our Monte Carlo simulation and the previous experiment [27] that we report in Fig. 3 is strikingly good for most dilution levels (up to and including $x = 1.7$ for $Dy_{2-x}Y_xTi_2O_7$) and over a rather wide temperature range $T \sim [0.5–5\ K]$. This is particularly noteworthy given that there is *no* adjustment of the microscopic parameters of the dipolar spin ice Hamiltonian of Eq. (2), except for the dilution of spins in the system. From these results, we conclude that a simple site-diluted version of the DSIM of Eq. (2) does capture the dilution physics of *both* materials at a quantitative level. This constitutes the first main result of this paper.

Close inspection of Fig. 3 shows that there is a discrepancy in $C_m(T)$ between simulation and experimental results for $T \gtrsim 5$ K. Also, the simulation results show a rise of $C_m(T)$ as T decreases below a temperature of approximately 0.4 K and 0.6 K for $Dy_{2-x}Y_xTi_2O_7$ and $Ho_{2-x}Y_xTi_2O_7$, respectively, while this behavior is barely noticeable in our experimental data. We address these two points in further detail in Sec. IV A, mostly at the phenomenological level, postponing the discussion of the physical implications of these results for the determination of the residual entropy to the following subsection. In Sec. IV B, we present the baseline low-temperature limit T_0 dependence of the residual entropy $S_{res}(T_0)$ as a function of dilution level x. We comment in Sec. IV C on the failure of our Monte Carlo simulations to reproduce the experimental results for $x = 1.8$ and 1.9.

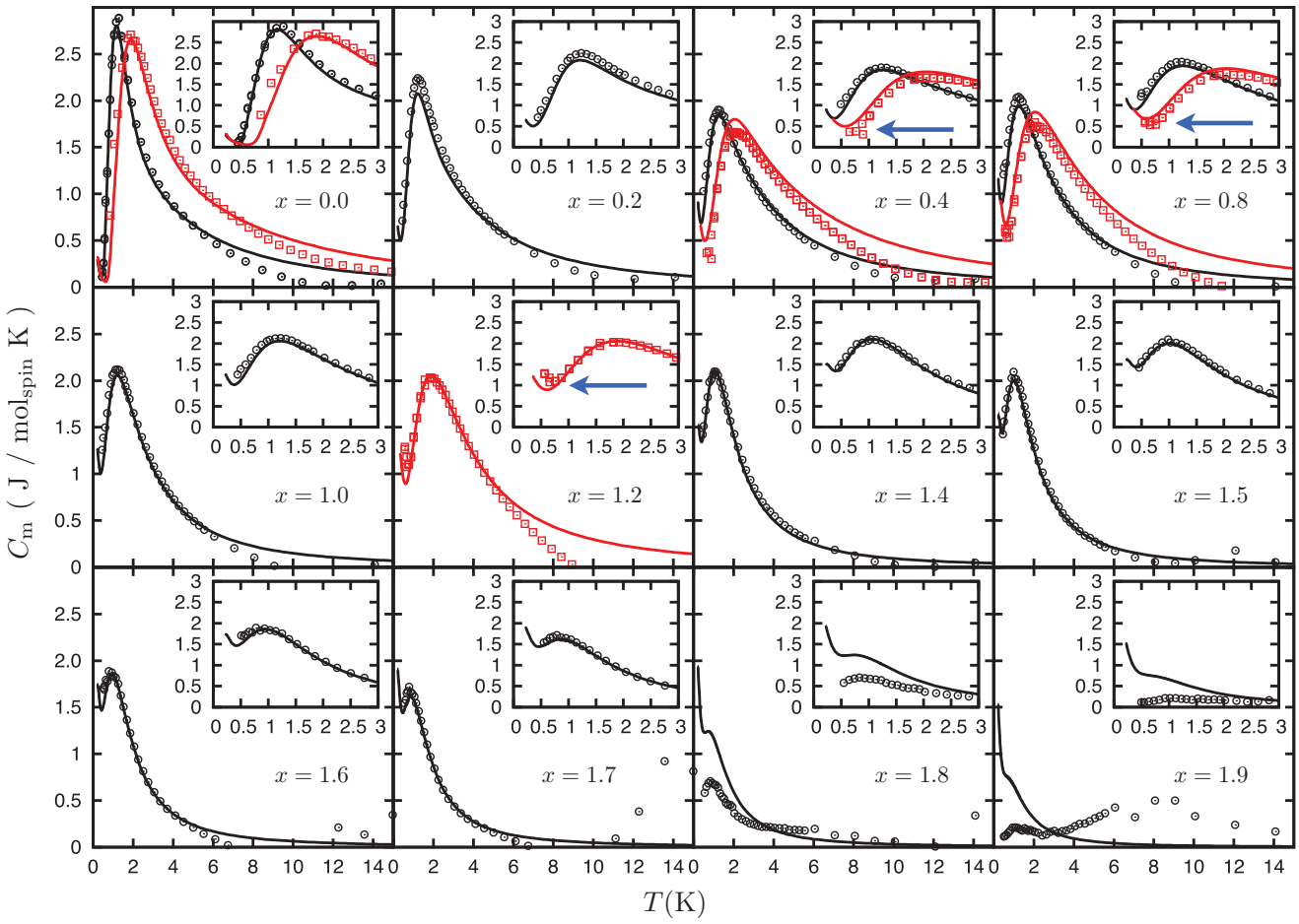

FIG. 3. (Color online) Comparison of the magnetic specific heat $C_m(T)$ between Monte Carlo simulations and experiments. Black open circles are for $Dy_{2-x}Y_xTi_2O_7$ experiment, solid black curves are for $Dy_{2-x}Y_xTi_2O_7$ simulations. Red open squares are for $Ho_{2-x}Y_xTi_2O_7$ experiment, and solid red curves are for $Ho_{2-x}Y_xTi_2O_7$ simulations. Insets show an enlargement around the Schottky peak at T_p, arising from the formation of the spin ice state. The horizontal blue arrows indicate location of $C_m(T)$ minima that may be occurring in $Ho_{2-x}Y_xTi_2O_7$.

A. High- and low-temperature regimes

1. High-temperature regime

In the "high-temperature regime," typically above 4 to 5 K, we observe that our simulation results for $C_m(T)$ depart from the experimental results. Such discrepancies need clarification since (i) a demonstration of the validity of the microscopic models considered depends on achieving a good degree of agreement between experimental and Monte Carlo $C_m(T)$ curves and since (ii) as we shall see when discussing the residual entropy in the next subsection, $C_m(T)$ for $T \gtrsim 5$ K contributes up to about 10% of the full R ln(2) magnetic entropy.

From a high-temperature expansion perspective, the magnetic specific heat is expected to follow a $C_m(T) \sim 1/T^2$ form at temperatures large compared to the typical temperature scale $T^{peak}(x)$, the temperature at which the specific heat peaks, set by the interactions in these systems. This form was indeed verified in all our simulation results. In contrast, all the experimental $C_m(T)$ data decrease at $T \gtrsim 5$ K significantly faster and are obviously not in agreement with this necessary $1/T^2$ high-temperature form.

We believe this fast dropoff in the experimental data is likely due to the oversubtraction of the lattice contribution to the total specific heat at these temperatures. The usual method for carrying out such a subtraction relies on an estimated Debye contribution for the acoustic phonons. For example, by considering the temperature range of 10 K $\leqslant T \leqslant$ 20 K, one might try to fit the total specific heat to the form $C_{total}(T) = A/T^2 + BT^3$, where the $1/T^2$ part comes from the aforementioned magnetic contribution and T^3 part is the Debye phonon contribution. Unfortunately, for $T \gtrsim 10$ K, background contributions from other components of the experimental setup become significant (see Sec. II). In particular, we note that in order to facilitate thermal conduction in the measurements, Ag powder was mixed into the spin ice powder samples. At these higher temperatures, the specific-heat contribution from the Ag component becomes larger than the magnetic component that we are trying to isolate. Fitting the phonon contribution with all these high-temperature background contributions embeds errors in the A and B fitting parameters, which then causes an oversubtraction for the magnetic specific heat $C_m(T)$ at $T \gtrsim 5$ K.

2. Low-temperature regime

We now turn to the low-temperature regime of the $C_m(T)$ curves, below the prominent peak at $T = T^{peak}$, with $T^{peak} \sim 1$ K for $Dy_{2-x}Y_xTi_2O_7$ and $T^{peak} \sim 1.9$ K for $Ho_{2-x}Y_xTi_2O_7$.

In particular, we discuss the minima found in the simulation results for all dilution levels (including $x = 0$, although in this case the minimum is more subtle [33,34]) in both the Dy and Ho spin ices (see solid curves in insets in Fig. 3). We note here that the value of C_m at its minimum value is not very different with that reported in the recent measurements of Ref. [26]. We find for $Dy_{2-x}Y_xTi_2O_7$ ($x = 0.2$) a minimum $C_m \sim 0.5$ J/(mol K) value at $T \sim 0.5$ K, which is close to the $C_m/T \sim 1$ J/(mol K^2) found, also, at $T \sim 0.5$ K in Ref. [26]. As discussed in Sec. IV B, the integrated entropy of the system is highly dependent on the $C_m(T)$ results at low temperatures since $dS = \frac{C_m(T)}{T} dT$.

It is known that in simulations of the undiluted dipolar spin ice model [33,34], a $C_m(T)$ minimum arises from the development of extra correlations within the spin ice state caused by the dipolar interactions, with the system eventually undergoing a transition to long-range order at $T_c \sim 0.13D$ ($T_c \sim 0.18$ K for the D value appropriate for $Ho_2Ti_2O_7$ [33,34]). For such a minimum to be found in undiluted spin ice simulations, collective spin update algorithms (loop moves discussed in Sec. III B) have to be included. On the other hand, it is very difficult for experiments to display such a $C_m(T)$ minimum and the long-range order transition, due to the freezing of spins below a temperature $T \sim 0.5$ K [26,35].

As discussed in Sec. III B, equilibrium in the simulations cannot be achieved without using collective update algorithms, further supplemented by parallel tempering. For $Dy_{2-x}Y_xTi_2O_7$, having used a ^{3}He cryostat (see Sec. II B), the experiments stop at temperatures just above the simulation-predicted minima. For $Ho_{2-x}Y_xTi_2O_7$, the $C_m(T)$ minima are perhaps experimentally observed (see horizontal blue arrows in the insets of Fig. 3 for $x = 0.4$, 0.8, and 1.2), although the experimental data points below the minima do not agree very well with the simulation results. In this case, one should be warned that there is a large nuclear contribution at $T \lesssim 0.5$ K for $Ho_2Ti_2O_7$ [28]. Even though this nuclear component has been subtracted (see Sec. II), its existence nevertheless complicates the possible experimental observation of the minima in the magnetic-only part $C_m(T)$ of the total specific heat $C(T)$.

While the present experimental data do not allow for a convincing observation of the minima in $C_m(T)$, we unquestionably find them in the Monte Carlo simulations of the microscopic DISMs. The minima observed in the specific-heat simulations of the diluted DSIMs acquire a significant value, as seen in Fig. 3, as opposed to the vanishing values in the undiluted variants (see $x = 0$ panel in Fig. 3) [33,34,45]. Furthermore, the broad specific-heat peak at $T^{peak}(x)$, which signals the development of ice-rule correlations as in the undiluted Dy and Ho spin ices, is less well defined in the presence of dilution. For example, for $x = 1.7$, the peak is more of a shallow hump feature resulting from a slight drop at about 0.4 K on the rising low-temperature ($T \leqslant 0.4$ K) portion of the $C_m(T)$ curve. Indeed, at such a high dilution, the ice rules are marginally enforced and the $C(T)$ peak associated with the development of ice rules fulfilling tetrahedra is not very prominent. As discussed further in Sec. IV B regarding the determination of the residual entropy $S_{res}(T_0)$ at a low temperature T_0, the behavior of the $C_m(T)$ curves suggests that the residual entropy concept employed for undiluted spin ices *cannot* be readily discussed without a specification of the lowest temperature T_0 at which (equilibrated) experimental data are obtained.

To sum up, there exist experimental difficulties in determining the magnetic-only contribution to the specific heat $C_m(T)$ in the high-temperature regime ($T \gtrsim 5$ K). For the low-temperature regime ($T \lesssim 0.5$ K), in contrast to the undiluted case, the $C_m(T)$ curves from our simulations display clear minima with significant $C_m(T)$ values. On the experimental front, these minima may be marginally observed in $Ho_{2-x}Y_xTi_2O_7$ ($x = 0.4, 0.8, 1.2$), but are not observed in $Dy_{2-x}Y_xTi_2O_7$. At the same time, the very good agreement between the experimental and Monte Carlo $C_m(T)$ for both materials (for x up to $x = 1.8$ for $Dy_{2-x}Y_xTi_2O_7$) and for 0.5 K $\lesssim T \lesssim$ 5 K seemingly vindicates the applicability of a simple site-diluted version of the DSIM to describe $Dy_{2-x}Y_xTi_2O_7$ and $Ho_{2-x}Y_xTi_2O_7$. This conclusion is best illustrated by considering the good agreement between experimental and Monte Carlo data for $C_m^{peak}(x)$ and $T^{peak}(x)$ in Fig. 2. In other words, the Ising nature of the Dy^{3+} and Ho^{3+} magnetic moment, along with the predominant classical energy scales of the Hamiltonian of Eq. (2), appear largely unaffected by the substitution of the magnetic rare-earth ions by nonmagnetic Y^{3+}.

In what follows, we thus take the following approach. Having demonstrated good agreement between experiments and models in the temperature range $T \sim$ [0.5–5 K] for both $Dy_{2-x}Y_xTi_2O_7$ and $Ho_{2-x}Y_xTi_2O_7$, in order to remedy the aforementioned experimental caveats, we henceforth only consider the *simulation data* of Eq. (2) to expose accurately what would be the "theoretically expected" (or, ideally experimentally determined) x dependence of the low-temperature residual entropy $S_{res}(x, T_0)$ of the $Dy_{2-x}Y_xTi_2O_7$ and $Ho_{2-x}Y_xTi_2O_7$ diluted dipolar spin ice materials.

B. Nonmonotonic residual entropy

1. Current analysis

Since Eq. (2) is an Ising model, the entropy at infinite temperature per mole of spin is R ln 2. Thus, the residual entropy $S_{res}(T_0)$ at a given temperature T_0 can be written as

$$S_{res}(T_0) = \mathrm{R} \ln 2 - \int_{T_0}^{\infty} \frac{C_m(T)}{T} dT. \quad (5)$$

We compute $S_{res}(T_0)$ obtained from the Monte Carlo simulations $C_m(T)$ data for different choices of T_0, where the integration to infinite temperature is done by fitting the $C_m(T)$ curves at high temperatures (>10 K) to a $1/T^2$ form.

The results from these Monte Carlo determinations of the residual entropy $S_{res}(T_0)$ are shown in Fig. 4 for both $Dy_{2-x}Y_xTi_2O_7$ and $Ho_{2-x}Y_xTi_2O_7$. We confirm the previous observation made by Ke *et al.* in Ref. [27] that there does exist (i) a nonmonotonic x dependence of $S_{res}(T_0)$ and (ii) that there is a difference in $S_{res}(T_0)$ between the two materials.

The main new result here is, thanks to the ability of the Monte Carlo simulations to provide accurate $C_m(T)$ data for the $T \lesssim 0.5$ K and $T \gtrsim 10$ K ranges, that we can now robustly expose both the x dependence and the materials dependence of $S_{res}(x)$. Supplementing the previous paper [27], we are

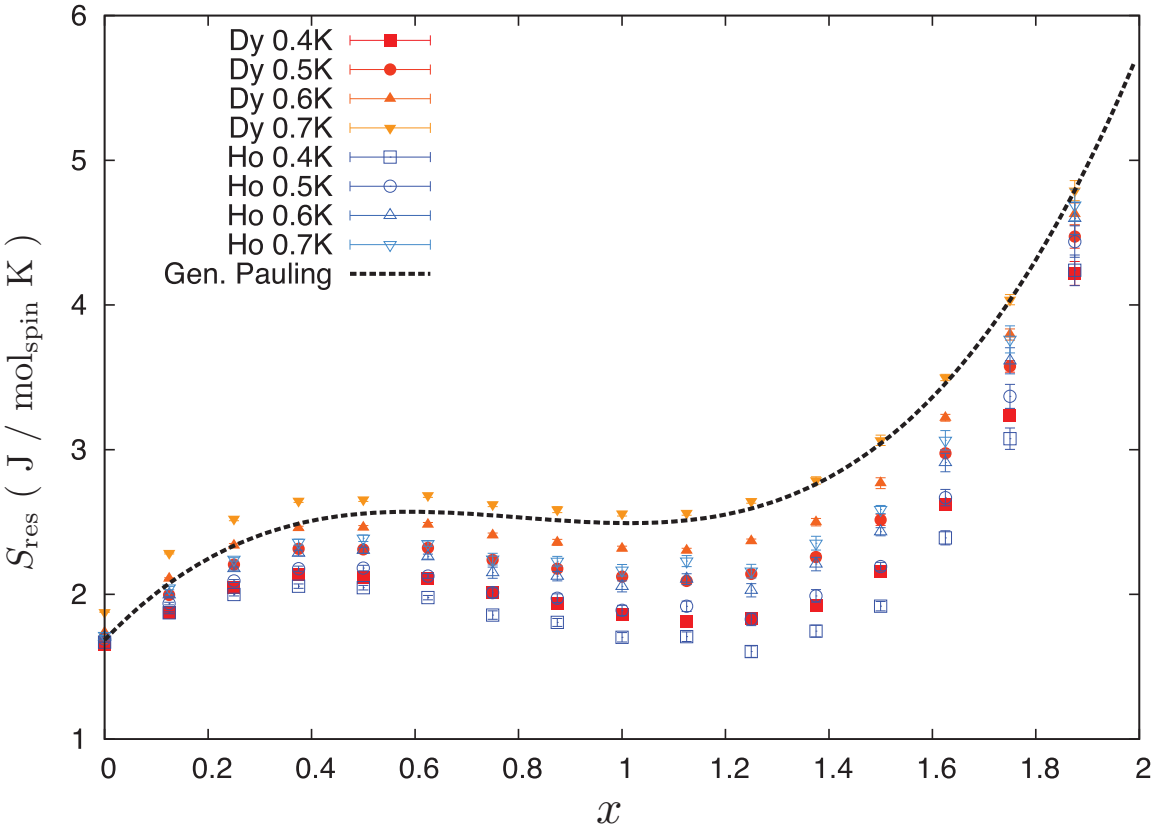

FIG. 4. (Color online) Residual entropy determined from Monte Carlo simulations for both $Dy_{2-x}Y_xTi_2O_7$ and $Ho_{2-x}Y_xTi_2O_7$ with different low-temperature limits T_0. The dotted black curve shows S_{res} given by the generalized Pauling's argument (gPa).

now also uncovering the importance of specifying the base temperature T_0 used in the determination of $S_{res}(x)$. Such a need to specify T_0 does not arise in previous works on undiluted $Dy_2Ti_2O_7$ and $Ho_2Ti_2O_7$ because $C_m(T)$ practically drops to zero near $T \sim 0.4$ K and S_{res} remains close to the Pauling value for $C_m(T)/T$ integrated upward anywhere from $0.45^{+0.10}_{-0.15}$ K (see, however, Ref. [26]). In particular, as a final and crucial observation, we note that for all values of x and for a given T_0, $S_{res}(x)$ is *lower* for $Ho_{2-x}Y_xTi_2O_7$ than for $Dy_{2-x}Y_xTi_2O_7$, in contrast to the conclusion that was reached in Ref. [27] and reproduced in Fig. 1.

To reiterate, as can be seen in Fig. 4, the results of the residual entropy for the diluted ($x > 0$) DSIM depend strongly on the choice of T_0, in contrast to the undiluted case ($x = 0$), in which the $S_{res}(T_0)$ for different T_0's almost collapse onto the calculation of the Pauling's entropy $(R/2)\ln(\frac{3}{2})$. For $x = 0$, the collapse of the $S_{res}(T_0)$ for different T_0's is the manifestation of the *projective equivalence* [31,32], which states that the quasi-ground-state properties of the DSIM can be described by an effective nearest-neighbor spin ice model up to corrections falling off as $1/r^5$. But, for $x > 0$, the T_0 dependence suggests an inconsistency with projective equivalence when site dilution is considered.

2. *Discussion and relation with the work of Ref. [27]*

At this juncture, it is perhaps useful to discuss the relationship between the results obtained here (see Fig. 4) and the ones reported in Ref. [27] (see Fig. 1). Considering the results in Fig. 4 for $Dy_{2-x}Y_xTi_2O_7$ and $Ho_{2-x}Y_xTi_2O_7$, we find that for a fixed T_0, both materials display a nonmonotonous dependence of $S_{res}(x,T_0)$ upon x. The overall nonmonotonous trend of $S_{res}(x,T_0)$, being roughly captured by the gPa, suggests some remnant of the physics of the diluted nearest-neighbor spin ice model within the diluted DISM. Yet, the two materials, because of their different magnetic interactions, do display quantitatively different $S_{res}(x,T_0)$ from each other and from the gPa. Specifically, the two series of compounds possess a different energy scale for the dipolar interaction D relative to the nearest-neighbor scale J_1, reflected in the values $J_{eff} = 1.06$ K for $Dy_2Ti_2O_7$ and $J_{eff} = 1.83$ K for $Ho_2Ti_2O_7$. Consequently, $Ho_{2-x}Y_xTi_2O_7$ enters the spin ice regime at a higher temperature than $Dy_{2-x}Y_xTi_2O_7$, as signaled by the temperature location of the peak in the specific-heat temperature $T^{peak}(x)$. Since $Ho_{2-x}Y_xTi_2O_7$ develops spin ice correlations at higher temperature than $Dy_{2-x}Y_xTi_2O_7$, it therefore displays a lower residual entropy $S_{res}(x,T_0)$ than the latter *for all* x and for the *same* (chosen) T_0 for both compounds. For example, referring to Fig. 4, we see that for a given x the $S_{res}(x,T_0)$ value is always lower for $Ho_{2-x}Y_xTi_2O_7$ than for $Dy_{2-x}Y_xTi_2O_7$ for a set T_0 value. Here, we are implicitly assuming that the system is cooled slowly from a temperature $T \gg T^{peak}(x)$ down to T_0 and that the determined $S_{res}(x,T_0)$ is an equilibrium thermodynamic value. Being a statement about an equilibrium measurement of $S_{res}(x,T_0)$, the above assertions are therefore not concerned about what the properties of the system are for $T < T_0$. This would be

the case whether the system freezes out of equilibrium in an ice-rule-obeying state, has a spin-glass state induced by a small amount of oxygen vacancies [55], marches towards a phase transition to long-range order [33,34], or is beginning to enter a coherent quantum spin ice regime [51,52], any of them possibly suggested by the recently reported rise of $C_{\rm m}(T)$ for $T \leqslant 0.5$ K [26].

The results displayed in Fig. 4 are different from those shown in Fig. 1 and which, as stated in the Introduction, largely motivated this work. In particular, the vertical ordering of $S_{\rm res}(x,T_0)$ of $Ho_{2-x}Y_xTi_2O_7$ versus $Dy_{2-x}Y_xTi_2O_7$ is swapped when going from Figs. 1 to 4. Let us explain the reasons for this. First, as discussed above and as illustrated in Fig. 3, the Monte Carlo results are in good agreement with experimental data for $Ho_{2-x}Y_xTi_2O_7$ and $Dy_{2-x}Y_xTi_2O_7$ over the temperature range [0.5,5.0] K. Consequently, if we were to compute the magnetic entropy $S_{\rm m}$ from both the experimental and Monte Carlo $C_{\rm m}(T)$ data defined over that same temperature range for both compounds ($S_{\rm m} = \int_{0.5}^{5.0} C_{\rm m} T^{-1} dT$), one would obviously find the same entropy within experimental uncertainty. There is therefore no mystery. One now recalls that the results reported in Fig. 4 are from Monte Carlo $C_{\rm m}$ results used to compute $S_{\rm res}(x,T_0)$ between a fixed T_0 and infinite temperature. As explained above, this procedure was followed because of the experimental difficulties in accurately extracting $C_{\rm m}(T)$ for $T \gtrsim 5.0$ K. In particular, the experimentally estimated $C_{\rm m}(T)$ for $T > 5.0$ K can fall significantly below the required $1/T^2$ dependence (e.g. see $x = 1.2$ panel in Fig. 4). The results from Ref. [27], reproduced in Fig. 1, having been obtained upon integrating the $C_{\rm m}(T)$ data from (i) a slightly varying baseline $T_0 = 0.45^{+0.05}_{-0.15}$ K and (ii) up to the maximum temperature (as large as 10 K), with $C_{\rm m}(T)$ determined after the Ag and lattice contributions having been subtracted, lead to an underestimated $S_{\rm res}(x)$, in particular for $Ho_{2-x}Y_xTi_2O_7$ (see the experimental $C_{\rm m}(T)$ data for $x = 0.4$, 0.8, and 1.2 for $T \gtrsim 5.0$ K in Fig. 3).

We thus consider the data shown in Fig. 1 now fully rationalized, and that these should be viewed as superseded by those of Fig. 4 as a more accurate reflection of the residual magnetic entropy at a baseline temperature T_0 in $Ho_{2-x}Y_xTi_2O_7$ and $Dy_{2-x}Y_xTi_2O_7$. This is the second main result of this paper.

C. Large level of dilution

It is perhaps remarkable that the nice agreement found between Monte Carlo simulations and experiments shown in Fig. 3 for $Dy_{2-x}Y_xTi_2O_7$ for $0 < x \leqslant 1.7$ disappears abruptly and essentially completely going from $x = 1.7$ to 1.8 and 1.9 (see Fig. 3). The only similarity left is that both Monte Carlo and experimental $C_{\rm m}(T)$ data show a low-temperature hump at a temperature $T \sim 0.8$ K (see insets of Fig. 3 for $x = 1.8$ and 1.9, which are further reproduced in Fig. 5). This figure further illustrates that despite the large dilution of magnetic ions for $x = 1.8$ and 1.9, finite-size effects remain negligible. By considering 1000 disorder realizations for $L = 3$, 4, and 5, we have also checked that the sample-to-sample variation is well bounded and the specific-heat data are therefore self-averaged. We are thus rather confident that the discrepancy between simulation and experimental results does not arise from computational pitfalls, but is a genuine physical difference.

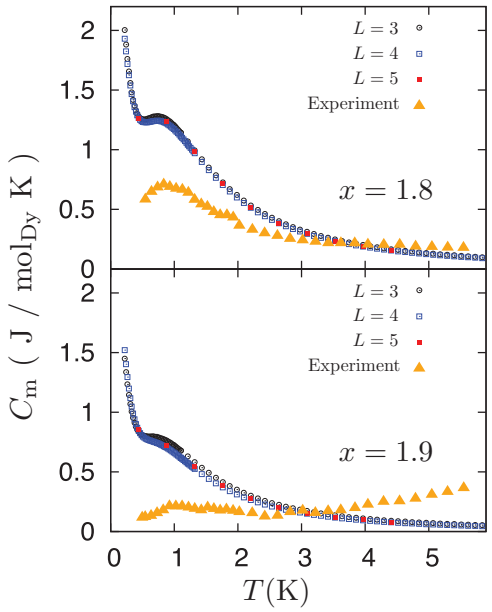

FIG. 5. (Color online) Comparison of Monte Carlo specific heat with experimental results for $Dy_{2-x}Y_xTi_2O_7$ for sizes $L = 3,4,5$ for $x = 1.8$ (top panel) and $x = 1.9$ (bottom panel). For these simulations, 1000 disorder realizations were considered to carry out the disorder average in Eq. (3).

Presently, we do not have a good suggestion as to what may cause such a sudden (in terms of "just" going from $x = 1.7$ to 1.8) and large discrepancy between experiments and Monte Carlo data. A possible mechanism includes the development of a dipolar Ising spin-glass state [38–41,43] inhibiting thermal equilibrium in the experiments. However, this should not be at play at temperatures as high as 1 K as we would naively expect the thermodynamic spin-glass transition temperature to be below 200 mK or so for those two concentrations [41,43]. Another possibility includes a significant random local lattice distortion developing upon reaching large levels of dilution. This would affect the J_ν couplings and the crystal field, hence, the magnetic moment μ and the dipolar coupling D compared to the values determined for $x = 0$. A third possibility is that of a highly uneven distribution of the magnetic ions as $x \to 2$. These last two possibilities would seem rather unlikely given the close ionic radius of Y^{3+} with Dy^{3+} and Ho^{3+} and the solid solution that exists in the whole $x \in [0,2]$ range. In this context, we note that no such concern has arisen in studies of the site-diluted $LiHo_{1-x}Y_xF_4$ dipolar Ising material, over the whole x range spanning the diluted ferromagnetic regime all the way to the spin-glass one [42,43]. More experiments are definitely required to understand the $x \to 2$ behavior of diluted spin ice materials.

V. CONCLUSION

Spin ice is at the present time one of the best understood highly frustrated magnetic systems, both from a microscopic model perspective [16,28,29,45] as well as from a field theoretic one [47–49,56]. Spin ices thus appear to be ideal systems to investigate quantitatively the effects of random disorder in a highly frustrated magnetic setting [49,56,57]. In this paper, we reported results from Monte Carlo simulations

of a site-diluted version of the dipolar spin ice model (DSIM) given by Eq. (2) for $Dy_{2-x}Y_xTi_2O_7$ and $Ho_{2-x}Y_xTi_2O_7$. A close match between simulation results and experiments for the magnetic specific heat $C_m(T)$ in the temperature range $0.5\ \text{K} \lesssim T \lesssim 5\ \text{K}$ was found up to, and including, $x = 1.7$ (85% magnetic ions diluted) for $Dy_{2-x}Y_xTi_2O_7$. This good agreement between simulations and experiments validates further the underlying dipolar spin ice models for these two compounds [28,45]. Specifically, that the Dy^{3+} and Ho^{3+} magnetic moments remain well described by a classical Ising variable and that the exchange couplings J_v and dipolar coupling constant D that enter the spin Hamiltonian of Eq. (2) are not significantly renormalized by the substitution of the rare-earth ion by Y^{3+}.

The nonmonotonicity of the residual entropy as a function of dilution levels $S_{res}(x,T_0)$ is confirmed to originate from the material-specific spin-spin interactions. Namely, it is due to the relative strength of the dipolar interactions with respect to the (mostly) nearest-neighbor exchange coupling J_1. Furthermore, despite the importance of specifying the base temperature T_0 from which thermodynamic integration of the magnetic specific heat $C_m(T)/T$ is carried out, $S_{res}(x,T_0)$ is nevertheless found to be roughly qualitatively described by a generalized version of the Pauling's approximation (gPa) to estimate $S_{res}(T_0)$. In summary, the difference in the residual entropy S_{res} between $Dy_{2-x}Y_xTi_2O_7$ and $Ho_{2-x}Y_xTi_2O_7$, as well as with the gPa, have been resolved in this work.

Encouraged by the robustness of the site-diluted dipolar spin ice model to describe the experimental observations for temperatures higher than 0.5 K or so, we hope that our work will stimulate further experimental investigations and theoretical studies of spin ice materials at $T \lesssim 0.5$ K, in particular in the context of evincing a possible transition to long-range order [26,33,34], a spin glass ground state [58] or a quantum spin ice state [51,52]. It would be interesting to explore further the highly diluted regime of $Dy_{2-x}Y_xTi_2O_7$ ($x \geqslant 1.8$) to clarify the origin of the discrepancy between experimental and Monte Carlo specific-heat data in that regime. It might also be interesting to explore the possibility of a dipolar Ising spin-glass state in the highly diluted regime of spin ice materials [57]. Definite progress in understanding dipolar Ising spin glasses has recently been made [38,41,43]. Other problems of disorder are relevant for spin ices, for example, evidence [37,59] that, in image furnace grown single crystals, there is a small level [$O(1\%)$] of substitution of the Ti^{4+} transition-metal ions by trivalent rare-earth ions, a phenomenon referred to as "stuffing" [60]. Other examples of disorder include the mixing of different types of ions on the rare-earth site [61], different nonmagnetic ions at the B site [62,63], and oxygen vacancies [55]. Thus, in comparison with these various forms of disorder, which would all generate random bonds [58], the problem of site dilution may be expected to be simpler, and a necessary first step in our broad goal of understanding the effects of random disorder in magnetic pyrochlore oxides [6].

Generally speaking, we expect the effects of disorder on the thermodynamic properties of other highly frustrated magnetic systems, such as the kagome materials $SrCr_xGa_{12-x}O_{19}$ (SCGO) [64–67] and $ZnCu_3(OH)_6Cl_2$ (herbertsmithite) [68,69], to attract ever growing interest. This is motivated by the necessity to understand whether the observed experimental behavior in SCGO and the putative quantum spin-liquid herbersmithite are intrinsic to the hypothetical disorder-free material or are, instead, strongly affected by disorder effects. The problem of site dilution in spin ice materials finds a natural place within this broad topic of random disorder in highly frustrated magnetic systems [7] and our work is a contribution to this research theme.

Note added in proof. Recently, a study by Sen and Moessner [57] investigates the importance of the ice rules on the dipolar spin glass freezing in a model of site-diluted dipolar spin ice model and refers to the underlying low-temperature state as a "topological spin glass."

ACKNOWLEDGMENTS

We thank L. Jaubert, P. McClarty, R. Moessner, S. Singer, P. Stasiak, and K.-M. Tam for helpful discussions. The authors gratefully acknowledge the group of Robert Cava at Princeton for sample preparation that enabled the original study of the samples discussed in the present work. This research was funded by the NSERC of Canada and the Canada Research Chair program (M.G. Tier I, R.G.M., Tier II), the Canada Foundation for Innovation (CFI), and the Ontario Innovation Trust (OIT). We acknowledge the use of the computing facilities of the Shared Hierarchical Academic Research Computing Network (SHARCNET:www.sharcnet.ca). P.S. acknowledges support of NSF Grants No. DMR-0701582 and No. DMR-1341793. X.K. gratefully acknowledges the partial financial support by the Clifford G. Shull Fellowship at ORNL. Research at the Perimeter Institute is supported by the Government of Canada through Industry Canada and by the Province of Ontario through the Ministry of Economic Development & Innovation.

[1] A. P. Ramirez, Annu. Rev. Mater. Sci. **24**, 453 (1994).
[2] H. T. Diep, *Frustrated Spin Systems* (World Scientific, Singapore, 2004).
[3] S. T. Bramwell and M. J. P. Gingras, Science **294**, 1495 (2001).
[4] C. Lacroix, P. Mendels, and F. Mila, *Introduction to Frustrated Magnetism* (Springer, Berlin, 2011).
[5] L. Balents, Nature (London) **464**, 199 (2010).
[6] J. S. Gardner, M. J. P. Gingras, and J. E. Greedan, Rev. Mod. Phys. **82**, 53 (2010).
[7] J. Villain, Z. Phys. B **33**, 31 (1979).
[8] M. J. Harris, S. T. Bramwell, D. F. McMorrow, T. Zeiske, and K. W. Godfrey, Phys. Rev. Lett. **79**, 2554 (1997).
[9] A. P. Ramirez, A. Hayashi, R. J. Cava, R. Siddharthan, and B. S. Shastry, Nature (London) **399**, 333 (1999).
[10] X. Ke, B. G. Ueland, D. V. West, M. L. Dahlberg, R. J. Cava, and P. Schiffer, Phys. Rev. B **76**, 214413 (2007).
[11] H. Kadowaki, Y. Ishii, K. Matsuhira, and Y. Hinatsu, Phys. Rev. B **65**, 144421 (2002).

[12] H. D. Zhou, S. T. Bramwell, J. G. Cheng, C. R. Wiebe, G. Li, L. Balicas, J. A. Bloxsom, H. J. Silverstein, J. S. Zhou, J. B. Goodenough *et al.*, Nat. Commun. **2**, 478 (2011).

[13] H. D. Zhou, J. G. Cheng, A. M. Hallas, C. R. Wiebe, G. Li, L. Balicas, J. S. Zhou, J. B. Goodenough, J. S. Gardner, and E. S. Choi, Phys. Rev. Lett. **108**, 207206 (2012).

[14] J. Lago, I. Živković, B. Z. Malkin, J. Rodriguez Fernandez, P. Ghigna, P. Dalmas de Réotier, A. Yaouanc, and T. Rojo, Phys. Rev. Lett. **104**, 247203 (2010).

[15] S. Rosenkranz, A. P. Ramirez, A. Hayashi, R. J. Cava, R. Siddharthan, and B. S. Shastry, J. Appl. Phys. **87**, 5914 (2000).

[16] M. J. P. Gingras, in *Spin Ice in Highly Frustrated Magnetism*, edited by C. Lacroix, P. Mendels, and F. Mila, Springer Series in Solid-State Sciences Vol. 164 (Springer, Berlin, 2011).

[17] L. Pauling, J. Am. Chem. Soc. **57**, 2680 (1935).

[18] O. Cépas and B. Canals, Phys. Rev. B **86**, 024434 (2012).

[19] W. F. Giauque and M. F. Ashley, Phys. Rev. **43**, 81 (1933).

[20] W. F. Giauque and J. W. Stout, J. Am. Chem. Soc. **58**, 1144 (1936).

[21] Y. Tajima, T. Matsuo, and H. Suga, Nature (London) **299**, 810 (1982).

[22] Y. Tajima, T. Matsuo, and H. Suga, J. Phys. Chem. Solids **45**, 1135 (1984).

[23] Singer, in *Hydrogen-Bond Topology and Proton Ordering in Ice and Water Clusters* (Wiley, New York, 2011), pp. 1–74.

[24] A. L. Cornelius and J. S. Gardner, Phys. Rev. B **64**, 060406 (2001).

[25] G. Prando, P. Carretta, S. R. Giblin, J. Lago, S. Pin, and P. Ghigna, in *Highly Frustrated Magnetism 2008 (HFM 2008)*, edited by I. Eremin, W. Brenig, R. Kremer, and J. Litterst (IOP, Bristol, 2009) [J. Phys.: Conf. Ser. **145**, 012033 (2009)].

[26] D. Pomaranski, L. R. Yaraskavitch, S. Meng, K. A. Ross, H. M. L. Noad, H. A. Dabkowska, B. D. Gaulin, and J. B. Kycia, Nat. Phys. **9**, 353 (2013).

[27] X. Ke, R. S. Freitas, B. G. Ueland, G. C. Lau, M. L. Dahlberg, R. J. Cava, R. Moessner, and P. Schiffer, Phys. Rev. Lett. **99**, 137203 (2007).

[28] S. T. Bramwell, M. J. Harris, B. C. den Hertog, M. J. P. Gingras, J. S. Gardner, D. F. McMorrow, A. R. Wildes, A. L. Cornelius, J. D. M. Champion, R. G. Melko *et al.*, Phys. Rev. Lett. **87**, 047205 (2001).

[29] B. C. den Hertog and M. J. P. Gingras, Phys. Rev. Lett. **84**, 3430 (2000).

[30] M. J. P. Gingras and B. C. den Hertog, Can. J. Phys. **79**, 1339 (2001).

[31] S. V. Isakov, R. Moessner, and S. L. Sondhi, Phys. Rev. Lett. **95**, 217201 (2005).

[32] C. Castelnovo, R. Moessner, and S. L. Sondhi, Nature (London) **451**, 42 (2008).

[33] R. G. Melko, B. C. den Hertog, and M. J. P. Gingras, Phys. Rev. Lett. **87**, 067203 (2001).

[34] R. G. Melko and M. J. P. Gingras, J. Phys.: Condens. Matter **16**, R1277 (2004).

[35] H. Fukazawa, R. G. Melko, R. Higashinaka, Y. Maeno, and M. J. P. Gingras, Phys. Rev. B **65**, 054410 (2002).

[36] C. Castelnovo, R. Moessner, and S. L. Sondhi, Phys. Rev. Lett. **104**, 107201 (2010).

[37] H. M. Revell, L. R. Yaraskavitch, J. D. Mason, K. A. Ross, H. M. L. Noad, H. A. Dabkowska, B. D. Gaulin, P. Henelius, and J. B. Kycia, Nat. Phys. **9**, 34 (2013).

[38] J. A. Quilliam, S. Meng, and J. B. Kycia, Phys. Rev. B **85**, 184415 (2012).

[39] A. Biltmo and P. Henelius, Phys. Rev. B **76**, 054423 (2007).

[40] A. Biltmo and P. Henelius, Phys. Rev. B **78**, 054437 (2008).

[41] K.-M. Tam and M. J. P. Gingras, Phys. Rev. Lett. **103**, 087202 (2009).

[42] M. J. P. Gingras and P. Henelius, in *International Conference on Frustration in Condensed Matter (ICFCM)*, edited by H. A. Katori, H. Kawamura, T. H. Arima, and S. Fujiyama, MEXT Project (IOP, Bristol, 2011) [J. Phys.: Conf. Ser. **320**, 012001 (2011)].

[43] J. C. Andresen, H. G. Katzgraber, V. Oganesyan, and M. Schechter, Phys. Rev. X **4**, 041016 (2014).

[44] L. J. Chang, Y. Su, Y.-J. Kao, Y. Z. Chou, R. Mittal, H. Schneider, T. Brückel, G. Balakrishnan, and M. R. Lees, Phys. Rev. B **82**, 172403 (2010).

[45] T. Yavors'kii, T. Fennell, M. J. P. Gingras, and S. T. Bramwell, Phys. Rev. Lett. **101**, 037204 (2008).

[46] R. R. P. Singh and J. Oitmaa, Phys. Rev. B **85**, 144414 (2012).

[47] C. L. Henley, Phys. Rev. B **71**, 014424 (2005).

[48] C. Henley, Annu. Rev. Condens. Matter Phys. **1**, 179 (2010).

[49] A. Sen, R. Moessner, and S. L. Sondhi, Phys. Rev. Lett. **110**, 107202 (2013).

[50] R. Siddharthan, B. S. Shastry, A. P. Ramirez, A. Hayashi, R. J. Cava, and S. Rosenkranz, Phys. Rev. Lett. **83**, 1854 (1999).

[51] L. Savary and L. Balents, Phys. Rev. Lett. **108**, 037202 (2012).

[52] M. J. P. Gingras and P. A. McClarty, Rep. Prog. Phys. **77**, 056501 (2014).

[53] Z. Wang and C. Holm, J. Chem. Phys. **115**, 6351 (2001).

[54] E. Marinari and G. Parisi, Europhys. Lett. **19**, 451 (1992).

[55] G. Sala, M. J. Gutmann, D. Prabhakaran, D. Pomaranski, C. Mitchelitis, J. B. Kycia, D. G. Porter, C. Castelnovo, and J. P. Goff, Nat. Mater. **13**, 488 (2014).

[56] A. Andreanov, J. T. Chalker, T. E. Saunders, and D. Sherrington, Phys. Rev. B **81**, 014406 (2010).

[57] A. Sen and R. Moessner, arXiv:1405.0668.

[58] L. Bellier-Castella, M. J. P. Gingras, P. C. W. Holdsworth, and R. Moessner, Can. J. Phys. **79**, 1365 (2001).

[59] K. A. Ross, T. Proffen, H. A. Dabkowska, J. A. Quilliam, L. R. Yaraskavitch, J. B. Kycia, and B. D. Gaulin, Phys. Rev. B **86**, 174424 (2012).

[60] G. C. Lau, R. S. Freitas, B. G. Ueland, B. D. Muegge, E. L. Duncan, P. Schiffer, and R. J. Cava, Nat. Phys. **2**, 249 (2006).

[61] H. Xing, M. He, C. Feng, H. Guo, H. Zeng, and Z.-A. Xu, Phys. Rev. B **81**, 134426 (2010).

[62] P. Bonville, J. A. Hodges, E. Bertin, J.-P. Bouchaud, P. Dalmas de Réotier, L.-P. Regnault, H. M. Rønnow, J.-P. Sanchez, S. Sosin, and A. Yaouanc, Hyp. Int. **156–157**, 103 (2004).

[63] M. L. Dahlberg, M. J. Matthews, P. Jiramongkolchai, R. J. Cava, and P. Schiffer, Phys. Rev. B **83**, 140410 (2011).

[64] A. P. Ramirez, G. P. Espinosa, and A. S. Cooper, Phys. Rev. Lett. **64**, 2070 (1990).

[65] P. Schiffer and I. Daruka, Phys. Rev. B **56**, 13712 (1997).

[66] A. Sen, K. Damle, and R. Moessner, Phys. Rev. Lett. **106**, 127203 (2011).

[67] I. Klich, S.-H. Lee, and K. Iida, Nat. Commun. **5**, 3497 (2014).

[68] P. Mendels and F. Bert, J. Phys.: Conf. Ser. **320**, 012004 (2011).

[69] T. Imai, M. Fu, T. H. Han, and Y. S. Lee, Phys. Rev. B **84**, 020411 (2011).